Available online at www.sciencedirect.com

ScienceDirect

Soils and Foundations 60 (2020) 1371–1386

www.elsevier.com/locate/sandf

Technical Paper

Development of geosynthetic-reinforced soil embankment resistant to severe earthquakes and prolonged overflows due to tsunamis

Kenji Watanabe [a,*], Susumu Nakajima [b], Kimihiro Fujii [c], Kosuke Matsuura [d], Atsuhiro Kudo [e], Takahiro Nonaka [f], Yudai Aoyagi [g,1]

[a] *University of Tokyo, 7-3-1, Bunkyo-ku, Hongo, Tokyo, Japan*
[b] *Railway Technical Research Institute, 2-8-38, Hikari-cho, Kokubunji-shi, Tokyo 185-8540, Japan*
[c] *JR West Japan Consultants Company, Japan*
[d] *Obayashi Corporation, Japan*
[e] *JR East Consultants Company, Japan*
[f] *Tokyu Construction, Japan*
[g] *Tokyo University of Science, Japan*

Received 23 March 2020; received in revised form 8 July 2020; accepted 5 August 2020
Available online 16 October 2020

Abstract

Many railway embankments sustained extensive damage due to the tsunami triggered by the 2011 off the Pacific Coast of Tohoku Earthquake, and the operations of several railway lines were suspended for an extended period of time.

Numerous studies have been conducted on enhancing the earthquake resistance of embankments, and this has led to the wide application of geosynthetic-reinforced soil (GRS) structures. However, only a few studies have been conducted on enhancing the tsunami resistance of embankments.

Based on onsite surveys and wave model experiments, the authors concluded that the damage to embankments was mainly caused by the large-scale earthquake occurring prior to the onset of the tsunami, and by the prolonged tsunami overflows that eroded the embankment bodies and the supporting ground.

In this study, therefore, two types of model tests were performed in order to propose a sturdy tsunami-resistant soil structure that exhibits ductile behavior against an earthquake prior to the onset of a tsunami as well as against prolonged overflowing.

It was confirmed that conventional embankments with sufficient seismic stability can be rapidly eroded by overflowing. On the other hand, the GRS method was found to be very effective for resisting the erosion of embankments due to overflowing.

Furthermore, given that the collapse of river dikes and levees due to overflows is often reported during heavy rainfall events, the findings obtained in the study are considered applicable to embankments as well as to river dikes and levees.

Keywords: Embankment; Geotextile; Overflow; Erosion; Earthquake; Tsunami; Model tests

1. Introduction

Railway embankments sustained extensive damage (runoffs and erosion) from the tsunami triggered by the 2011 off the Pacific Coast of Tohoku Earthquake, and operations of several railway lines were suspended for an extended period

Peer review under responsibility of The Japanese Geotechnical Society.
* Corresponding author.
E-mail addresses: watanabe@civil.t.u-tokyo.ac.jp (K. Watanabe), nakajima.susumu.99@rtri.or.jp (S. Nakajima), fujii_k@jrnc.co.jp (K. Fujii), matsuura.kosuke@obayashi.co.jp (K. Matsuura), a-kudo@jrc.jregroup.ne.jp (A. Kudo), nonaka.takahiro@tokyu-cnst.co.jp (T. Nonaka), aoyagi-y573ck@pwri.go.jp (Y. Aoyagi).
[1] Currently Public Works Research Institute.

https://doi.org/10.1016/j.sandf.2020.08.006
0038-0806/

of time (Koseki et al., 2012; Japanese Geotechnical Society, 2011).

The authors conducted an analysis based on onsite surveys and wave model experiments and concluded that the damage was primarily caused in the sequence described below (Fig. 1, Watanabe et al., 2017).

1. The main structures and protective surfaces (embankment bodies) of railway embankments sustained damage from the earthquake prior to the onset of the tsunami.
2. The tsunami occurred when the structures were already in a damaged condition, the embankments were eroded by the prolonged tsunami overflows, and uplift pressure acted on the protective surfaces.
3. The water overflowing from the embankments eroded the supporting ground around the lower sections of the embankments (toes of the slopes) on the inland side, and this further destabilized the embankments.

Several studies have focused on enhancing the earthquake resistance of railway embankments based on critical damage caused by the Hyogo-ken Nanbu Earthquake of 1995. The critical damage seen after the earthquake and a precise investigation of it led to the wide application of geosynthetic-reinforced soil structures (hereinafter referred to as "GRS" structures), using methods such as the "RRR Construction Method" developed by the Railway Technical Research Institute and University of Tokyo. Geotextiles are planar reinforcement materials composed of high polymer materials in lattice patterns (Fig. 2). They are used to increase the stability of earth structures when arranged horizontally in embankments. However, only a few studies have focused on enhancing the tsunami resistance of railway embankments.

In the current design standards for Japanese railway structures, the required performances and the performance indices under both seismic and non-seismic conditions are clearly defined (RTRI, 2007), although the required performance of railway structures against tsunamis is not defined. Furthermore, railway embankments in coastal regions are generally constructed on the inner side of coastal levees; and thus, these embankments are often expected to constitute secondary barriers (multiple protection) to curb the damage caused by tsunamis (prolonged overflows). Given the aforementioned points, it is important for railway embankments to exhibit sufficient stability and ductile behavior against prolonged tsunami overflows in a manner similar to coastal levees.

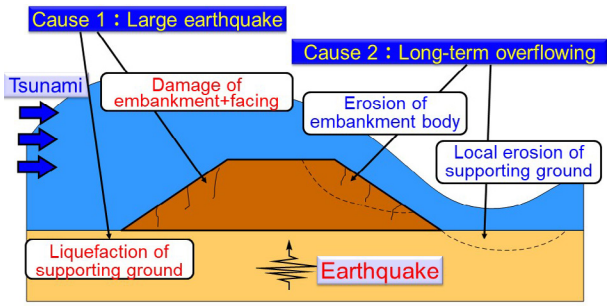

Fig. 1. Main cause of damage by Tsunami.

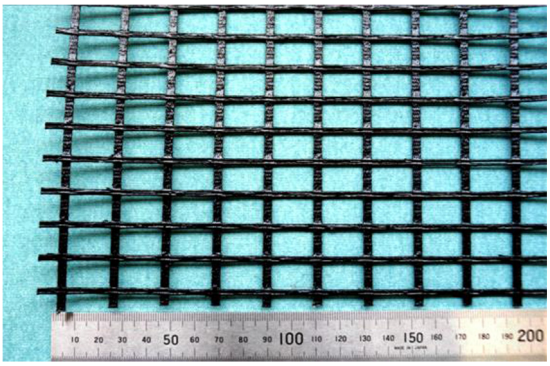

Fig. 2. Outlook of geotextile.

Several studies have focused on the erosion of embankments caused by overflowing or overtopping. Powledge et al. (1989a, 1989b) reported that erosion as a result of overflows during flood events is a principal cause of the failure of embankment dams and provided information on various protection systems developed to prevent the erosion of dams. Chevalier et al. (2014) summarized erosion phenomena in rivers and waterways in terms of "Hazard Type", "Research Approached", and "Disciplines", and reported that the erosion of embankments due to overflows during flood events corresponds to an important aspect of structural stability and safety. Lachaussée et al. (2016) performed overflowing model tests on an embankment composed of cohesive material and suggested that overflow first produces surface erosion at the toe of the downstream side of the embankment and erodes the profiles propagated upstream (regressive erosion), thereby increasing the hydraulic gradient, which is responsible for triggering piping erosion (hole erosion). Tabrizi et al. (2017) investigated the effects of soil compaction on the embankment breach process due to overtopping via experiments. The study focused on the degradation rate of an embankment breach for different levels of compaction, and non-dimensional relationships were developed for the height of the crest and the bottom length of the embankment as a function of time. Watanabe et al. (2014) performed large-scale wave maker tests to evaluate the water pressure and uplift force (negative pressure) acting on a rigid embankment model (400 mm in height). The experiment revealed that negative pressure continuously applied to the slope of the embankment (landward side) during steady overflow (Fig. 3), thereby indicating that negative pressure caused by overflowing induced strong erosion phenomena from the top corner of the embankment. However, because of the limitation of the total volume of water supply, only a short-term overflowing phenomenon was reproduced. It was deemed

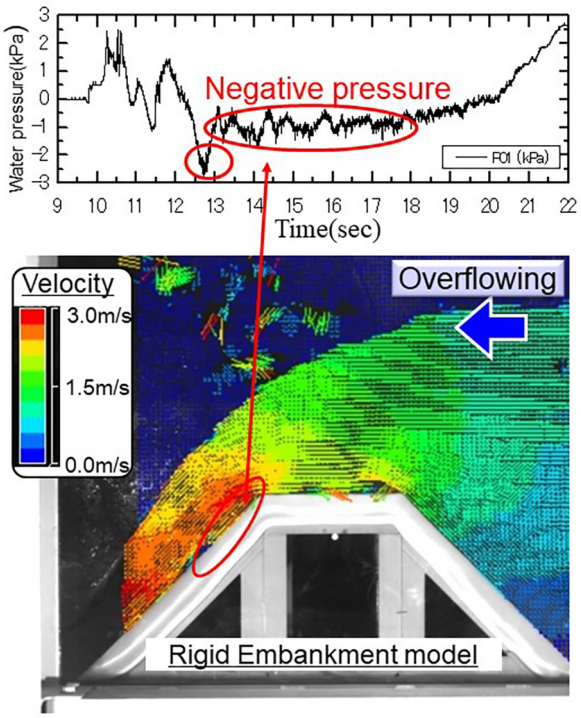

Fig. 3. Velocity distribution during overtopping obtained by high speed camera and PIV method.

necessary to perform another model test that focused on the resistance characteristics of the embankment against prolonged overflowing.

Only a few studies have focused on the resistance of GRS structures against overflowing. Matsushima et al. (2007) proposed protecting the downstream slope by using inclined soil bags anchored with geosynthetic reinforcement to increase the stability of small earth-fill dams against overflowing. Full-scale model tests on the hydraulic overflow-induced collapse of the downstream slope were performed and indicated that geosynthetic soil bags with extended tails (GSET) were sufficiently stable against overflow. Yamaguchi et al. (2013) performed overflowing model tests of tsunamis to evaluate the erosion resistance of reinforced-embankment models (100 mm in height). The experiments revealed that reinforcements arranged horizontally in an embankment effectively increased the durability of the embankment against a tsunami. However, only overflowing caused by step waves was reproduced in the model tests, and erosion caused by long-term overflowing was beyond the scope of the study.

In the present study, therefore, two types of model tests were performed to propose a sturdy tsunami-resistant soil structure that exhibits ductile behavior against an earthquake prior to the onset of a tsunami as well as against prolonged overflowing.

Firstly, a series of small-scale overflowing tests on both conventional and GRS types of small embankment models (100 mm in height) were performed, and the erosion properties of the embankments and the supporting ground during the overflowing as well as the effect of the geotextile were investigated. The material was carefully selected prior to conducting the small overflowing model tests.

Secondly, in addition to these basic small-scale model tests, a series of large-scale overflowing tests was performed. The authors installed a new water channel into the shaking table apparatus at the Railway Technical Research Institute in order to analyze the effect of a large-scale earthquake occurring prior to the onset of a tsunami as well as prolonged overflowing on the stability of the two types of embankment models (following the current seismic design standards of Japanese railways and both having a height of 400 mm). Prior to the overflowing experiment, shaking table tests with a high intensity of shaking (equivalent to Level 2 earthquake motion) were performed on the embankment models.

2. Selection of banking materials for experiments

2.1. Example of banking materials employed in past studies

Table 1 shows examples of the banking materials used in the model tests in previous studies. For example, three different uniform granular sands, having different degrees of apparent cohesion, were used for the river embankment model in the breaching and overtopping model tests performed by Pickert et al. (2011). Silica sand (D_{50} = 0.064–0.239 mm) was used in the overflowing model tests performed by Mizutani et al. (2012) in which the effect of the particle size and differences in the degree of saturation of the embankment on the overflowing erosion were precisely investigated. Sand with a larger diameter (D_{50} = 0.3 mm) was used in the model test performed by Hatogai et al. (2012) who examined the scouring at the bottom of the back slope. Suzuki et al. (2013) also used sand for a model test that focused on the erosion characteristics attributed to differences in the inclination of the slopes of the embankment model.

Conversely, a sandy loam was used by Yamamoto and Yoshino (1978) who indicated the relationship between the erosion rate and the dry density. Miyamoto et al. (2013) used silt-mixed sand in overflowing model tests. The tests indicated that the suction effect was higher for smaller particles when the embankment was unsaturated; and thus, the erosion decreased. There was barely any erosion due to overflowing on the front slope (seaward side), and the erosion of the crest and the maximum erosion depth on the crest and at the edge (toe) of the back slope were decreased by constructing the back slope gently. In addition, such factors as the flow rate, dry density of the backfill material, and water content at the beginning of the experiment were also observed to affect the erosion characteristics.

The objective of the present study is to examine the effect of the reinforcement (geotextile model) on the resistance to overflow through a model experiment. Given that various types of materials were adopted in previous studies

Table 1
List of embankment materials used in previous studies.

Literature	Material	D_{50} (mm)	k (cm/s)	w (%)
Pickert et al. (2011)	Fine sand	0.18		5.0
	Medium sand	0.34		5.0
	Coarse sand	0.6		5.0
Mizutani et al. (2012)	Silica sand No. 6 and No. 8	0.064–0.239	–	–
Hatogai et al. (2012)	Sandy soil	0.3	–	–
Suzuki et al. (2013)	Kiryu sand	–	3.1×10^{-4}	14.0–28.2
			2.35×10^{-4}	5.4–6.7
Yamamoto and Yoshino (1978)	Sandy loam	0.1	3.1×10^{-4}	14.0–28.2
Miyamoto et al. (2013)	Toyoura sand	–	–	–
	Mixture of Toyoura sand and silt	–	–	–

based on the focus of each study, it is difficult to select an appropriate material for the overflowing tests based only on the information provided in Table 1.

2.2. Key points to selecting banking materials for overflowing tests

When selecting the banking materials for the models that will simulate the deformation of the embankment caused by a large earthquake and erosion caused by prolonged overflowing, the following key points should be considered:

(1) Erosion resistance of the material
(2) Permeability of the material
(3) Seismic stability of the model embankment
(4) Ratio of the aperture size of the reinforcement (geotextile model) to the particle size of the material

It is difficult to select one banking material that can satisfy all the key points. Thus, in this study, different materials were used for the small-scale model tests, simulating only the overflows, and for the large-scale model tests, simulating a large earthquake and the overflows.

2.2.1. Material used for small-scale model tests

Bentonite-mixed sand was used in the small-scale model tests by considering points (1) and (2). This was based on the assumption that the embankment cannot be saturated within a short duration of overflowing, due to an actual tsunami, and that surface erosion, as opposed to the effect of water penetration or internal erosion from the seaward side, is the dominant factor in destabilizing the embankment. Therefore, in the small-scale model tests, banking material with lower permeability and lower resistance against erosion was considered as more suitable than that with higher permeability to qualitatively reproduce the actual failure process of the embankments due to overflowing. Moreover, materials used in real railway embankments generally exhibit cohesive strength; and thus, the use of ground material with some degree of cohesion was considered as suitable for qualitatively reproducing the process as it most closely resembles the actual phenomenon. Oda et al. (2007) used bentonite-mixed dry sand for the soil material to perform jet erosion experiments. They increased the weight ratio of bentonite to sand to show that the erosion rate decreases when the cohesive strength of the material increases.

Based on the knowledge gained from the aforementioned studies and the ease of the availability of the materials, a good blend of silica sand No. 6 (G_s = 2.652 and D_{50} = 0.237 mm) and No. 8 (G_s = 2.652 and D_{50} = 0.080 mm), to which bentonite was added to provide cohesive strength, was used as the banking material and to support the ground model. In order to determine the appropriate formulation of the materials and the ratio of the bentonite mixture that would provide the optimal banking material for the experiment, preliminary overflowing experiments were conducted using a small water channel. The experiments are described in Section 2.3.

2.2.2. Material used for large-scale model tests

Gravel was used for the large-scale model tests by considering points (3) and (4). The bentonite-mixed sand that was used for the small-scale model tests was not employed for the large-scale model tests because the particle size of the bentonite-mixed sand was significantly smaller than the aperture size of the reinforcement (geotextile model); and thus, sand particles were easily squeezed out from the aperture during overflowing. The behavior decreased the tensile strength mobilized in the reinforcement. It would not have been possible for this type of behavior to easily occur given the actual particle size of the banking material and the aperture size of real geotextile. Furthermore, shaking table tests were performed to evaluate the seismic stability of the embankment for the large-scale model tests; and thus, the seismic stability of a model embankment composed of bentonite-mixed sand would have become excessively high.

Another issue to consider when performing shaking table tests involves decreasing the friction between the earth structure model and the sidewalls of the soil container. Dry sand is typically used in most shaking table tests to minimize the sidewall friction. However, when constructing an earth structure model with cohesive material (e.g., bentonite-mixed sand), it is necessary to arrange a lubrication layer or to create a slight gap between the model and the sidewalls to decrease friction. However,

for large-scale model tests, in which shaking table tests and overflowing tests are performed continuously, a lubrication layer or slight gap between the model and the sidewalls could correspond to a "water path" and induce local erosion and destruction.

Given the above information, gravel was used for the large-scale overflowing model tests in consideration of points (3) and (4) and to decrease the sidewall friction. The actual railway embankment simulated in the model tests was composed of well-graded gravel (named M40 in the Japanese Industrial Standard, D_{max} = 40 mm and D_{50} = 7.6 mm) and the geotextile models were arranged horizontally for the GRS embankment. As 63.4% of the well-graded gravel (M40) passed through the aperture of actual geotextiles (aperture mesh size: approximately 12 × 21 mm), the banking material of the model embankment was obtained by sieving the M40 by 9.5 mm (D_{max} = 9.5 mm and D_{50} = 1.7 mm). Additionally, 61.9% of this sieved material passed through the aperture of the model geotextiles with an aperture mesh size of 3 × 4 mm.

Froude similitude is applicable to water flow phenomena; however, it is not applicable to erosion phenomena. Considering the similarity law for bed load transport, the ratio of the particle size of the model embankment material to that of the prototype should be the same as the model scale. In the case of the large-scale model tests, the ratio of the D_{50} of the model embankment to that of M40 (prototype material) is about 0.22, which does not match the model scale (1/10). However, since the ratio of the aperture size of the geotextile model to the particle size of the embankment material is more dominant for the erosion phenomena of GRS embankments, aforementioned point (4) was more strongly considered in this study.

2.3. Preliminary small-scale overflowing model tests for selecting appropriate formulation for banking material and ratio of bentonite mixture

2.3.1. Model preparation

Fig. 4 shows the model test configuration. A small water channel (1900 mm long, 350 mm high, and 300 mm wide) was used as the experimental device. Channel circulating water, produced by several submersible pumps, was used to reproduce the prolonged overflowing phenomenon caused by a tsunami to the maximum possible extent. An embankment model with a crest width of 75 mm and a height of 100 mm or with a crest width of 110 mm and a height of 150 mm, corresponding to a 1/40 or a 1/27 scale from the prototype embankment, was constructed in the water channel that was mounted horizontally. Reinforcement material was not used in the model tests to select the banking material.

The water level on the seaward side of the embankment was statically raised at a constant flow rate of 27.9 l/min. The time at which the water level reached the top slope of the seaward side was considered to be the starting time of the overflowing. The objective of the experiment was to observe the duration of overflowing and the erosion state of the embankment through the arrangement.

As shown in Table 2, the backfill material consisted of a mixture of dry silica sand No. 6 and No. 8 in the ratio 1:1 or 1:3 mixed with 1.0% to 3.0% by weight of bentonite.

2.3.2. Erosion characteristics of embankment among different types of material

Table 3 shows the erosion rate every 10 s for all cases. It is seen that the erosion rate corresponds to the ratio of the cross-sectional area of the eroded embankment (as observed from the transparent side of the channel) to the cross-sectional area of the embankment in the initial stage. In CASE 2, the embankment exhibited the highest resistance to erosion, although the backfill material formed masses (lumps) with a diameter of approximately 10 mm and peeled off because the ratio of the bentonite mixture was high. Therefore, lower ratios of bentonite mixture were used in CASES 4 and 6. In CASE 6, the fines content was increased to maintain the erosion resistance.

Two points were confirmed for CASES 4 and 6. Firstly, there was no distinct difference in the erosion processes between the two cases (Table 3), thereby indicating that increasing the fines content did not significantly affect the erosion resistance under the present experimental conditions. Secondly, the erosion of the surface in contact with

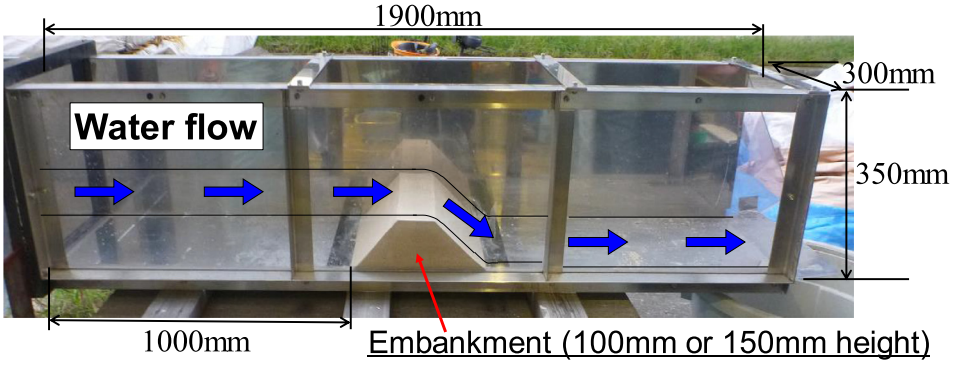

Fig. 4. Overview of small-scale overflowing model test.

Table 2
List of small-scale overflowing tests without reinforcement.

	CASE 2	CASE 4	CASE 6	CASE 10	CASE 15
Silica sand (No. 6 : No. 8)	1:1	1:1	1:3	1:1	1:1
D_{50} (mm)	0.133	0.133	0.092	0.133	0.133
Bentonite contents (%)	3.0	2.0	2.0	1.0	1.0
w (%)	20	20	20	20	15
ρ_d (g/cm^3)	1.59	1.54	1.54	1.54	1.57
Height (mm)	100	100	100	150	100
Curing days	–	–	–	2	0.5

Table 3
Erosion rate of each experiment.

Elapsed time	Erosion rate (%)				
	CASE 2	CASE 4	CASE 6	CASE 10	CASE 15
0 s	0.0	0.0	0.0	0.0	0.0
10 s	0.2	3.8	5.1	2.4	9.7
20 s	0.4	16.6	17.6	9.7	22.3
30 s	1.7	28.6	33.1	17.5	36.3

the sidewalls of the water channel increased when the overflow continued, although initially the erosion progressed evenly in the water channel. Hence, the central portion of the embankment remained as shown in Fig. 5.

In the model experiment, it was desirable to maintain uniform erosion throughout the width of the water channel, although erosion proceeded more from the sidewalls than from the central part of the embankment because the friction between the sidewalls of the water channel and the embankment was generally low. This is the reason why the central portion of the embankment was not eroded in CASE 4 (Fig. 5).

The above information suggests that it was necessary to further decrease the bentonite mixture. Therefore, in CASE 10, in addition to decreasing the ratio of the bentonite mixture, an attempt was made to maintain the erosion resistance by allowing for a few days of curing after creating the model. Thus, it could be ensured that the erosion proceeded evenly throughout the width of the waterway in CASE 10 where the bentonite proportion was 1% (Fig. 6). However, it was observed that the erosion in the crest was less than that in the back surface of the embankment. The erosion resistance of the embankment surface increased due to drying shrinkage during curing. Hence, there was barely any erosion in the crest region where the flow velocity was slow, while there was significant erosion in the back surface of the embankment where the flow velocity was high. Therefore, the curing time was decreased.

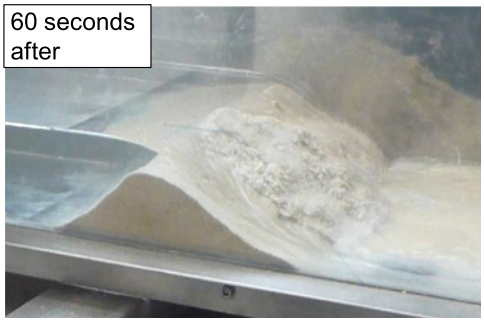

Fig. 5. Erosion of the embankment due to overflowing (CASE4).

2.3.3. Appropriate banking material for small overflow model tests

Based on the above-mentioned experimental results, a mixture of silica sand No. 6 and No. 8 was used in the ratio of 1:1, with 1.0% bentonite and curing for half a day as the banking material in the small-scale overflowing model tests. Furthermore, the dry density was fixed at $\rho_d = 1.57$ g/cm^3 (degree of compaction of $D_c = 95\%$ by the standard Proctor) and the water content was fixed at $w = 15\%$, which approximately corresponded to the optimum moisture content. Additionally, spray cement was applied to the front slope (seaward side) of the model, up to a thickness of approximately 1–2 mm, considering the prevention against water penetration of protective surface. It is usually arranged on the front surface of an actual embankment.

The results of the verification experiment conducted for the selected ground materials (CASE 15) are shown in Fig. 7. They show that erosion proceeded evenly in the width direction of the water channel. It is also observed in the figure that the erosion progressed uniformly in the crest and the back slope, and that water penetration was almost nonexistent along the front slope.

3. Small-scale overflowing model tests

3.1. Models for embankment and reinforcement

The height of the embankment was the same as that in the previous chapter (CASE 15), although the crest width was changed to 95 mm (Fig. 8). The models were constructed in the same water channel (Fig. 4). The embankment body was composed of bentonite-mixed silica sand, similar to Case 15 ($\rho_d = 1.57$ g/cm^3 and $w = w_{opt} = 15\%$), while well-graded gravel ($D_{max} = 4.75$ mm, $w = w_{opt} = 5\%$, and $\rho_d = 2.00$ g/cm^3) was used at the top layer (20 mm in height) of the GRS embankment (CASES 23 and 24) to reproduce the railway roadbed material. For comparison purposes, the top layer of CASE 21 was composed of

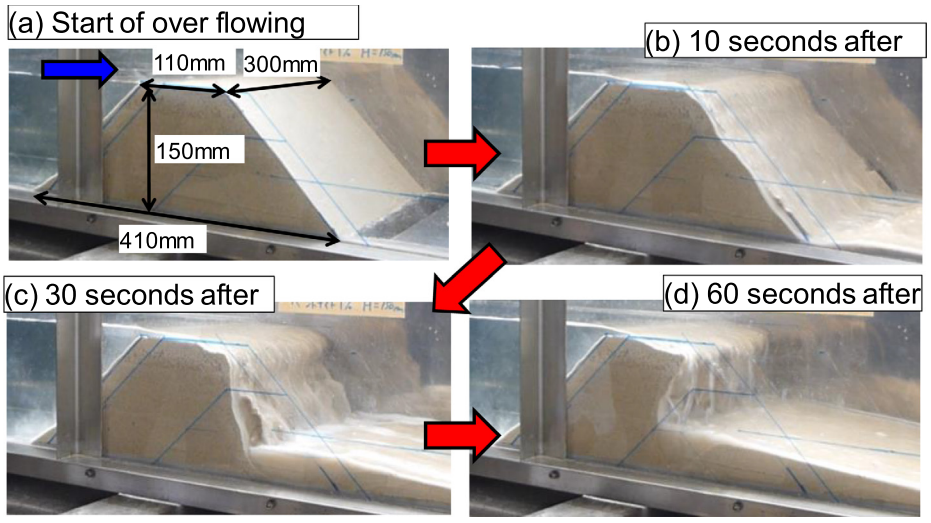

Fig. 6. Erosion of the embankment due to overflowing (CASE10).

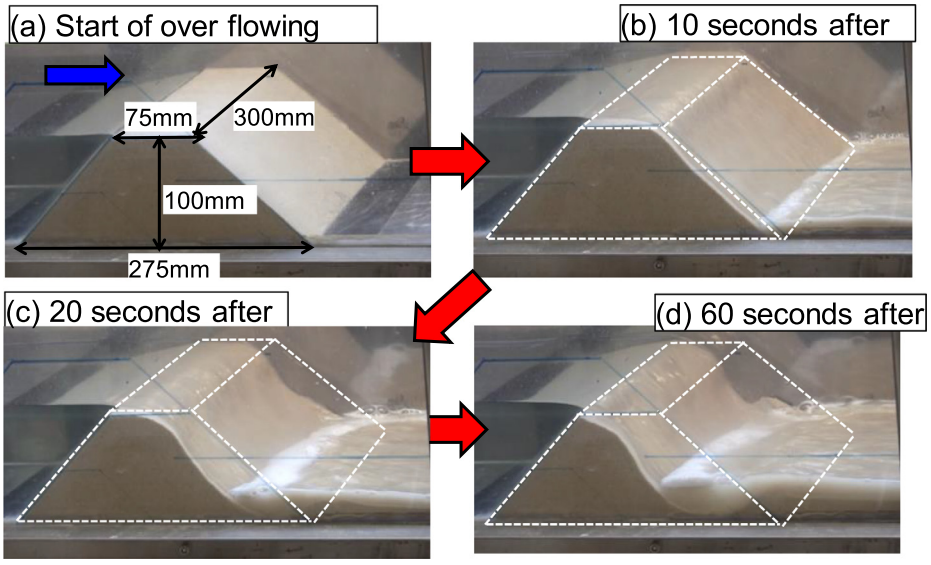

Fig. 7. Verification experiment conducted for the selected ground materials (CASE15).

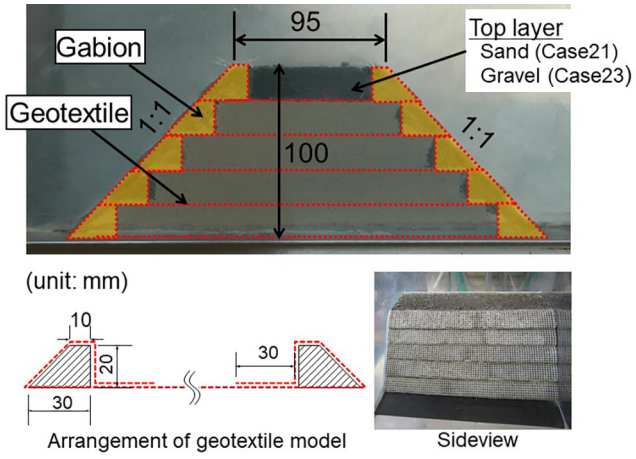

Fig. 8. GRS embankment model and arrangement of geotextile.

bentonite-mixed silica sand, which was identical to that of the embankment body. The compaction of the banking material was performed at intervals of 20 mm.

A polyester mesh sheet (aperture mesh size: approximately 3 × 4 mm) was used for the geotextile model for the GRS embankment (hereafter, referred to as the reinforcement). In accordance with the common practice for practical construction, the gabion model was arranged at both edges of the embankment of each layer, and the reinforcement was folded by rolling it around the gabions to a folded length of 50 mm (Fig. 8). In the arrangement of the gabions in the height direction at the site, it was important to obtain better contact between the upper and lower gabions such that sufficient frictional force would be mobilized. Hence, a trapezoidal gabion model was fabricated, and the contact surface between the upper and lower

gabions was secured. Moreover, the gabion model was designed to maintain water permeability.

A supporting ground model was constructed for CASES 25, 26, and 32 to investigate the effect of the erosion of the supporting ground on the stability of the GRS embankment. The material and compaction level for the supporting ground model were identical to those for the embankment body.

The reinforcement was installed in five layers. It was arranged entirely from the left to the right edges of the GRS embankment for CASES 21, 23, 25, 26, and 32, while a short reinforcement (60 mm in length) was arranged from both sides of the edges for CASE 24.

The water level on the seaward side of the embankment was statically raised by a flow rate corresponding to 27.9 l/min. When the embankment model was confirmed to be in a steady condition, the water supply was increased in a step-by-step manner by increasing the number of submersible pumps (up to six pumps) until the embankment collapsed. Employing such a method to increase the water supply stepwise, it became possible to compare the critical water flow against erosion among the embankment models. Table 4 shows the water flow rate of each step for all the tests, and Table 5 shows the overflow depth at each step above the seaward crest.

3.2. Effect of reinforcement on durability of embankment without supporting ground model

Fig. 9 shows the changes in the shape of the embankment model during overflowing, and Fig. 10 shows the retention rate of the cross-sectional area after the start of overflowing. The ratio corresponds to the cross-sectional area of the embankment at each stage relative to the cross-sectional area of the embankment at the initial stage; it was calculated from video images obtained from the front of the water channel. In CASE 15 (without reinforcement), erosion from the landside of the crest commenced immediately after the start of the overflowing. The erosion proceeded very rapidly, and more than half of the embankment body was eroded within 30 s.

Erosion from the top layer commenced in the early stage of CASE 21 where the top layer was composed of bentonite-mixed sand. Given the arrangement of the entire reinforcement, which was folded by rolling it around the gabions, it exhibited ductile behavior that significantly exceeded that of CASE 15, although the erosion proceeded rapidly after the flow out of the top gabion on the landward side. The results revealed that the stability of the gabions, which can be effectively increased by connecting them to the entire reinforcement, is one of the important factors in preventing erosion around the landward edge.

Table 4
Water flow rate of each step for all tests.

Step	Elapsed time	Flow rate (l/min)		
		CASE 15	CASE 21,23,24,25	CASE 26 &32
1	0 s ~ 20 s	27.9	23.0	23.2
2	20 s ~ 360 s	51.0	48.3	49.9
3	360 s ~ 480 s	–	113.5	116.9
4	480 s ~ 660 s	–	171.2	167.9
5	660 s ~ 900 s	–	236.4	234.3
6	900 s~	–	259.4	234.3

Table 5
Overflow depth above crest of embankment.

Step	Elapsed time	Overflow depth
1	0 s ~ 20 s	13 mm
2	20 s ~ 360 s	20 mm
3	360 s ~ 480 s	31 mm
4	480 s ~ 660 s	40 mm
5	660 s ~ 900 s	51 mm
6	900 s~	54 mm

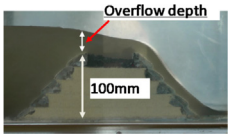

The GRS embankment with the entire reinforcement (CASE 23) was not eroded even after 300 s. Slight surface erosion at the top layer (gravel layer) and slight erosion at the second layer from the top were observed in the photo obtained at 1760 s (Fig. 9), but the embankment exhibited high stability and ductility.

The GRS embankment with a short reinforcement (CASE 24) also exhibited ductile behavior similar to that of CASE 23 until 600 s (Fig. 9). However, after the gabion model at the top layer (landward side) flowed out with a gravel layer at 690 s, erosion rapidly proceeded to the second layer that was composed of bentonite-mixed sand at 750 s, and the embankment exhibited brittle behavior.

The entire reinforcement, arranged from the left edge to the right edge of the embankment (CASE 23), prevented the progression of erosion in the vertical direction, and the tensile force mobilized in the entire reinforcement prevented the gabions from flowing out. However, the short reinforcement that was not connected from the left to right edges lost the tensile force mobilized in the reinforcement, following the erosion of the banking material above it (i.e., a decrease in confining pressure on the reinforcement). The results indicated that it is very effective to use the entire reinforcement and coarse material for the top layer of an embankment to increase the durability and restorability of the embankment against prolonged overflowing.

3.3. Effect of supporting ground erosion on stability of GRS embankment

3.3.1. GRS embankment on supporting ground model (without countermeasures)

The GRS embankment with the entire reinforcement was constructed on the supporting ground model 60 mm in depth (Fig. 11). The same material (bentonite-mixed sand) was used for the supporting ground model. The supporting ground model for CASE 25 was constructed without any countermeasures, although the ratio of the bentonite mixture was increased to 3% in "Region A" for

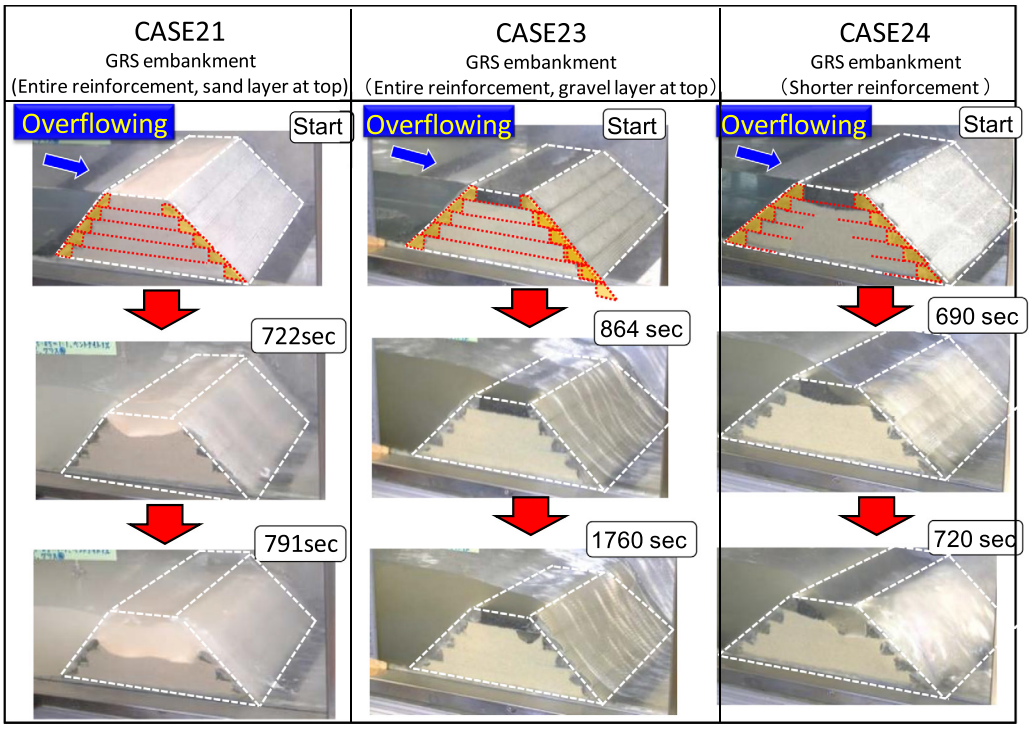

Fig. 9. Erosion of the GRS embankment.

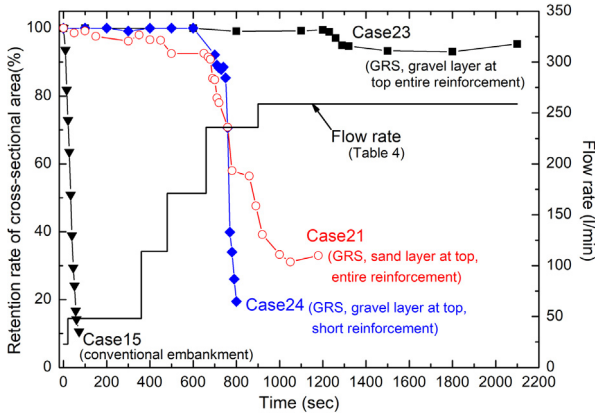

Fig. 10. Retention rate of cross-sectional area after the start of overflowing.

CASE 26, as seen in Fig. 11, and 2% of cement was added in the bentonite-mixed sand in "Region B" for CASE 32. The concept of these countermeasures is subsequently discussed.

As shown in Fig. 12, the reinforced embankment itself (CASE 25), constructed on the supporting ground model, exhibited high overflow resistance similar to that for CASE 23, described in the previous section. However, the supporting ground model was eroded from the embankment bottom tip of the landward side immediately after the experiment was started, and the erosion propagated to the ground directly under the embankment.

Furthermore, when the erosion of the supporting ground reached the bottom of the water channel, the erosion area expanded in the left and right directions. Subse-

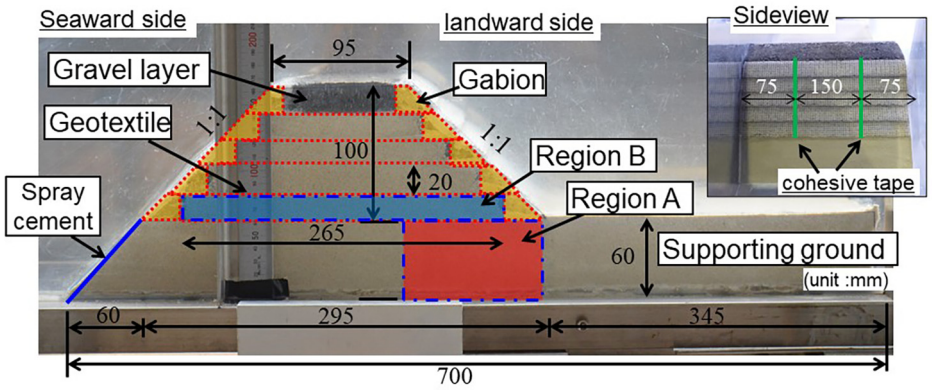

Fig. 11. GRS embankment model and bearing stratum model.

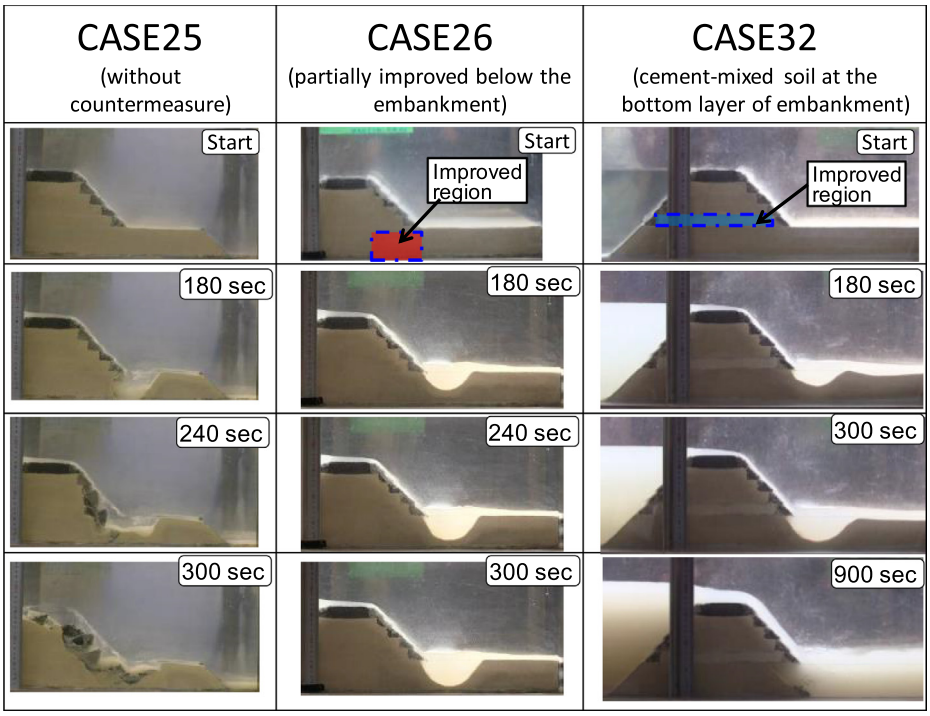

Fig. 12. Erosion of GRS embankment model constructed on supporting ground model.

quently, the gabion model at the bottom tip of the landward side tilted downward. 240 s from the start of the overflow, a gap was formed above the bottom gabion model, and the erosion of the embankment proceeded from the gap. After 300 s, the embankment exhibited a significant collapse.

The results indicated that the erosion of the supporting ground due to the overflow significantly affected the stability of the embankment. The test results are consistent with the cases of damage to sea embankments during the Tohoku Earthquake where significant erosion of the back slopes (landward side) was accompanied by the scour of the supporting ground at the edge of the back slopes (Tokida et al., 2012). Therefore, in order to develop an embankment that resists prolonged overflowing, it is important to improve the supporting ground as well as the embankment body.

3.3.2. *Countermeasures for supporting ground*

Ground improvements, including cement mixing for the whole supporting ground or the placing of vertical steel sheet piles from the toe end of an embankment, are often used as general countermeasures for the supporting ground. However, general countermeasures are very expensive because they need to be applied along the entire long length parallel to the railway embankment. Moreover, the land boundary of railways is generally limited to the embankment width, and this means that it is necessary to acquire additional land to improve the supporting ground outside the embankment.

Therefore, in the present study, further experiments with two different types of reasonable countermeasures were performed wherein cement improvement was applied to (1) the supporting ground below the embankment at the landward side (Region A in Fig. 11) and (2) the bottom layer of the embankment (Region B in Fig. 11).

The countermeasure applied to Region B (CASE 32) simulated the application of a "cement-mixed gravel soil slab". The slab was composed of crushed stone for mechanical stabilization with a small volume of cement. These slabs are frequently applied to earth structures to allow a limited degree of deformation. In the Japanese railway field, the materials correspond to a standardized type that is applicable to backfill material in the transition zone behind bridge abutments of a new Shinkansen line.

Laboratory tests and on-site tests revealed that the materials exhibited sufficient strength and deformation characteristics equivalent to concrete (Lohani et al., 2004). Therefore, a cement-mixed gravelly soil slab, with a geotextile arranged for the tensile material, was applicable as a bending member (e.g., a slab as a new type of countermeasure method for constructing railway embankments on soft grounds and liquefiable grounds).

This corresponds to a composite material of cement-mixed gravelly soil (compressive member, usually approximately 50 kg/m^3 of cement mixture) and the geogrid (tension member). Watanabe et al. (2011) indicated the high bending deformation characteristic of the composite material through bending load tests (Fig. 13), and the composite material was applied to an actual railway project in Japan

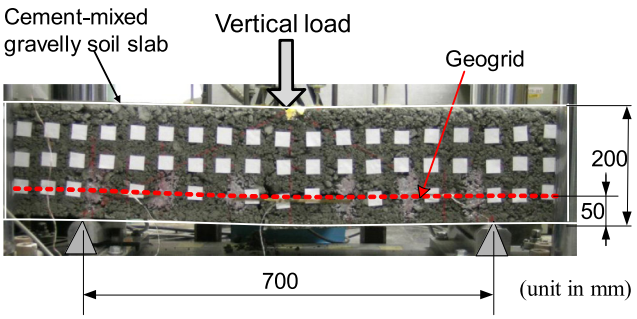

Fig. 13. Bending load test of cement-mixed gravelly soil slab with geogrid (Watanabe et al., 2011).

where the embankment (maximum height = 3.5 m and length = 110 m) was constructed on a weak cohesive soft ground and a liquefiable ground. Given that the composite material can be constructed in the same manner as an earth structure with sufficient compaction control and does not require any framework (e.g., construction work of concrete), the construction was completed in a considerably easier and faster manner than reinforced concrete. In the example, the ground improvement ratio for the cohesive soft ground was able to be decreased by almost half, and a large cost reduction was realized.

The model slab was applied to the bottom layer of the GRS embankment (CASE 32). The layer was composed of cement-mixed sand, and the geogrid reinforcement was not arranged inside the layer. Additionally, the gabions on the landward side were connected in the height direction by applying a thin cohesive tape from the surface of the gabions and assuming that simple slope work would be performed at the site.

3.3.3. GRS embankment for supporting ground model (with countermeasures)

Firstly, the photographs shown in Fig. 12 are used to compare CASE 25 corresponding to the GRS embankment without countermeasures and CASE 26 in which the supporting ground below the embankment on the landward side was improved. It is observed that, immediately after the start of the experiment, the erosion of the supporting ground below the bottom edge of the embankment (landward side) progressed at almost the same speed in both cases. However, the erosion of the ground improvement part for CASE 26 was limited even 180 s after the overflowing started when the bottom gabion (landward side) for CASE 25 collapsed, and the shape of the embankment was maintained even 300 s after the experiment commenced. The extent of the collapse observed 780 s after the experiment started in CASE 26 was identical to that observed 300 s after the experiment started in CASE 25.

Next, CASE 25 is compared to CASE 32 in which the bottom layer of the GRS embankment was improved and the gabion model was connected in the height direction. The erosion process in the initial stage was similar to that in CASE 25. However, in CASE 32, even when the erosion reached the supporting ground under the embankment, the gabion model did not collapse and no erosion of the embankment occurred. Thus, the GRS embankment maintained its height even 900 s after the overflow commenced and high overflow resistance was exhibited. This is because the shape of the embankment body was maintained by the slab applied to the bottom layer of the embankment and by connecting the gabions in the height direction. The collapse of the bottom gabion and the leakage of the embankment material due to the opening between the gabions were prevented.

3.4. Summary of small-scale overflowing model tests

In this chapter, a series of small-scale overflowing model tests was performed. The experiments revealed that the GRS method is effective for preventing the erosion of an embankment caused by overflowing and especially when the entire reinforcement is arranged horizontally from the left edge to the right edge of the embankment. The results also revealed that even partial improvement of the supporting ground immediately below the embankment and/or the application of a high-quality material or cement-mixed gravelly soil slab at the bottom layer of the embankment is very effective for stabilizing the embankment against overflowing.

The model tests in the chapter only reproduced the prolonged overflowing caused by a tsunami; the large earthquake prior to the onset of a tsunami was not reproduced. Hence, the model tests in the next chapter will reproduce the large earthquake that occurs prior to the tsunami by using a larger water channel on the shaking table apparatus.

4. Large-scale overflowing model tests on geosynthetic-reinforced soil embankment

4.1. Development of new tsunami experiment device and model preparation

An experimental device was developed that can reproduce large-scale earthquakes occurring prior to the onset

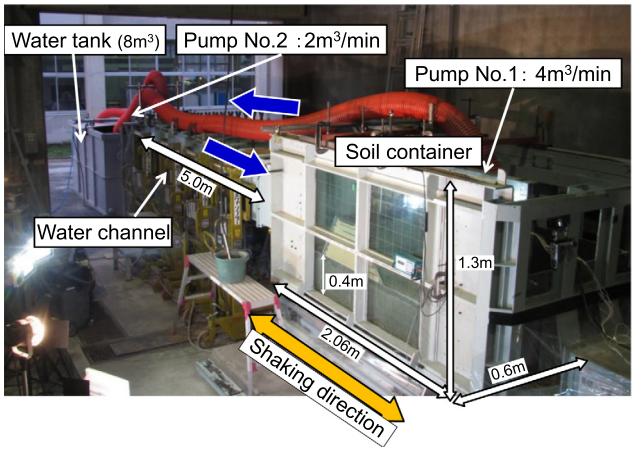

Fig. 14. Experimental apparatus for large-scale earthquake and prolonged overflow caused by Tsunami.

of a tsunami and the phenomenon of prolonged tsunami overflows (Fig. 14). The apparatus can circulate water at approximately 2 m^3/min via a water tank (capacity 8 m^3) by connecting a water channel (5.0 m long, 0.70 m high, and 0.60 m wide) to the side of a soil container on a shaking table apparatus. The soil container is 2.06 m long, 1.30 m high, and 0.60 m wide. The water channel is connected at a height of 400 mm from the bottom of the soil container; and thus, an embankment model can be constructed on a 400-mm-thick supporting ground model. The device does not reproduce the dynamic effects of waves, but can statically increase the water level on the seaward side of the embankment and maintain the overflow for a long time at a flow rate corresponding to 2 m^3/min. The apparatus can reproduce an overflow at a depth of approximately 130 mm at the crest of the embankment (seaward side) and a flow velocity of approximately 1.0 m/sec for a 1/10 scale embankment model with a height of 400 mm.

Fig. 15a shows a conventional railway embankment model (CASE A) with an earthquake-resistant design using better banking materials, sufficient compaction control, thickness control, and the arrangement of a short geogrid reinforcement 150 mm long (red dashed lines in Fig. 15a) at height intervals corresponding to 50 mm that are almost in compliance with the Railway Design Standard for Earth Structures (RTRI, 2007).

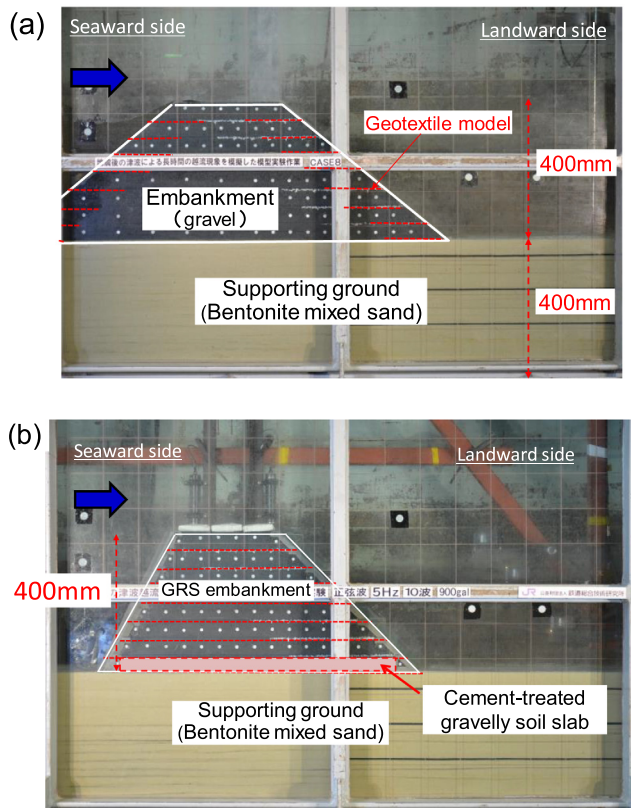

Fig. 15. Embankment model for large scale overflowing model test. (a) Conventional type embankment (CASE A). (b) GRS embankment (CASE B).

Conversely, Fig. 15b shows the GRS embankment model (CASE B). A polyester mesh sheet (composed of the same material as discussed in Chapter 3) was used as the geotextile model. This reinforcement was arranged at intervals corresponding to 50 mm. In addition, the bottom layer of the embankment was constructed with a "cement-mixed gravelly soil slab" composed of cement-mixed gravelly soil (q_u = 2000 kN/m^2) and a geogrid. The slab was applied to prevent the propagation of erosion from the supporting ground to the embankment body.

The inclination of the slope corresponded to 1:1.2 for the conventional type (CASE A), 1:0.5 on the seaward side of the GRS embankment (CASE B) with a rigid wall simulating a standard type of GRS retaining wall (RRR construction method), and 1:1 on the landward side with no slope protection. The reinforcement on the landward side was folded by rolling it around the gabion model to a folded length of 150 mm.

Firstly, large seismic loads were applied by horizontally shaking the soil container by sinusoidal base acceleration at a frequency of 5 Hz and approximately 20 cycles of waves. The initial base acceleration was first set at 200 Gal, which corresponds to a Level 1 earthquake in the current design standards for Japanese railway structures (RTRI, 2007), and was increased in increments of 200 Gal until 800 Gal. It was completed by applying 900 Gal of the sinusoidal wave. The maximum acceleration almost corresponds to a Level 2 earthquake in the current Japanese design standards which has to be considered for the seismic design of important earth structures.

After the shaking table tests, the models were subjected to prolonged overflow until the model collapsed.

4.2. Test results and discussion

4.2.1. Shaking table tests prior to a tsunami

Fig. 16 shows the response acceleration in the supporting ground and the top layer of the embankment (300 mm in height), and the horizontal and vertical displacements of the embankment at the crest for the last shaking step. It can be seen that the embankment exhibited dynamic fluctuation during shaking in both horizontal and vertical directions of around 0.1 mm to 0.4 mm. The residual displacement is very small, thereby confirming that the embankments exhibited sufficient earthquake resistance. It should be noted that the dynamic fluctuation of the horizontal displacement is larger for CASE B (GRS). This is because the inclination of the slope on both the seaward side and the landward side of the GRS embankment is steeper than that of a conventional embankment.

4.2.2. Overflowing tests after shaking table tests

Fig. 17a shows the erosion progress of the embankment and the supporting ground. It is observed that the conventional embankment (CASE A) rapidly eroded from the upper layer on the landward side and the erosion propagated from the supporting ground to the embankment

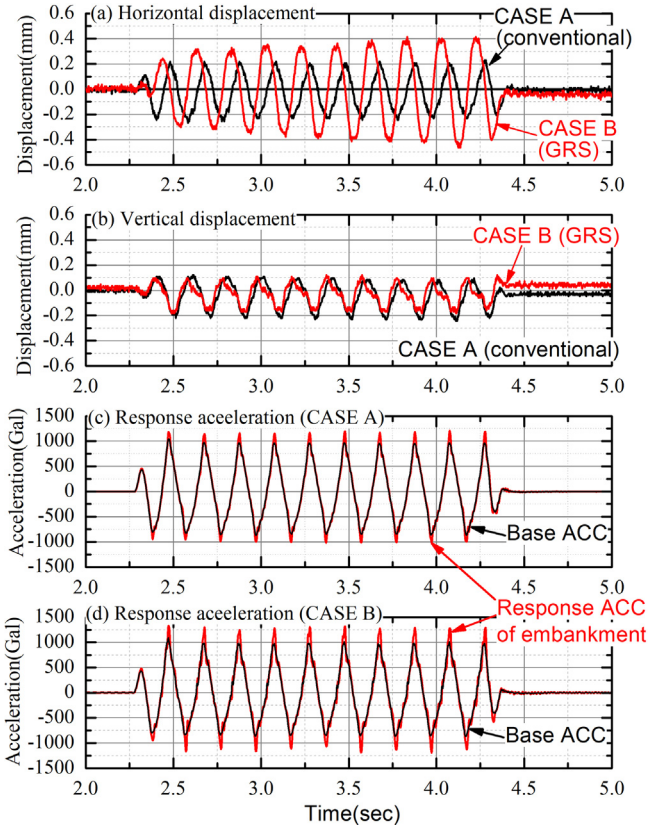

Fig. 16. Time history of acceleration and displacement of embankment during shaking table test.

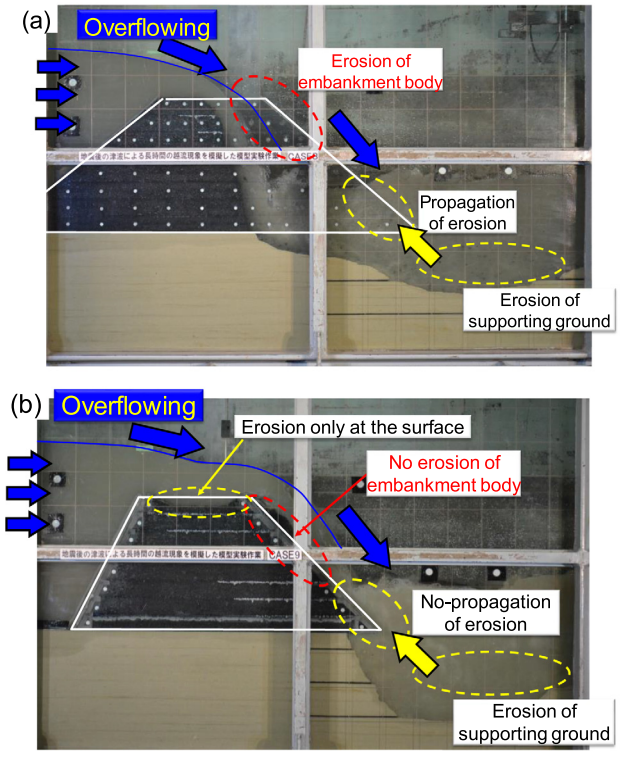

Fig. 17. Progress of erosion observed in the large-scale overflowing test (2 min after the overflow started). (a) Conventional type embankment (Case A). (b) GRS embankment (CASE B).

body. Approximately half of the banking embankment is eroded 2 min after the overflow started. Based on Froude similitude at a scale of 1:10 for the flow condition, this is equivalent to approximately 6 min on an actual scale. The results indicate that an embankment having sufficient seismic stability can be rapidly eroded by overflows.

Conversely, Fig. 17b shows that the GRS embankments (CASE B) are less likely to erode under tsunami overflows occurring over longer durations. Moreover, although the roadbed material of the top layer flowed out, erosion did not progress below the reinforcement at a depth of 5 cm from the surface. The results are different from those in which the erosion progressed more deeply than the installation position of the reinforcement in the small overflow experiment using bentonite-mixed sand (CASES 21 and 23). They depend on the relationship between the aperture size of the reinforcement and the particle size of the embankment material, thereby indicating that Point (4) in 2.2 is one of the most important indices when selecting the material for use in a GRS embankment model which will be subjected to erosion.

The erosion of the supporting ground on the landward side progressed immediately after the overflow started, as observed in CASE A. However, the edge (toe) of the embankment in CASE B was less likely to become unstable even under such conditions. This is mainly due to the bending stiffness of the cement-mixed gravely soil slab placed at the bottom layer of the GRS embankment.

Overflowing tests were continued for three minutes for CASE A and 10 min for CASE B (Fig. 18). Although more than the half the embankment body of the conventional type was eroded in three minutes, the GRS embankment maintained its stability and shape even after 10 min. This is equivalent to approximately 30 min on an actual scale, indicating the strong effect of the geotextile against erosion.

5. Recommendations for new geosynthetic-reinforced soil embankment and design procedure

5.1. Recommendations for new geosynthetics-reinforced soil embankment

Based on the experimental results, a new reinforced soil structure was proposed (Fig. 19). It exhibits sufficient stability and ductility against large-scale earthquakes, prolonged overflows caused by tsunamis, and the capacity to prevent embankments from becoming unstable due to the erosion of the supporting ground outside railway perimeters.

The required performance is primarily satisfied by using a GRS structure for the embankment to sustain large-scale earthquakes. The proposed structure corresponds to an improvement in the conventional GRS structure. In the structure, long strips of geotextile are arranged in the upper and lower layers of the embankment, which can readily be eroded by prolonged tsunami overflows, and are subsequently folded by rolling them around the gabions located

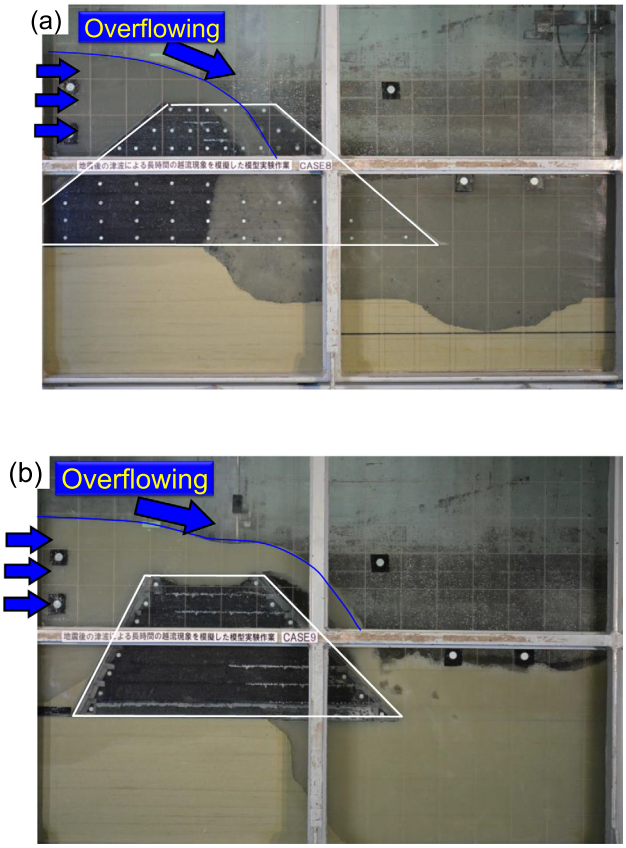

Fig. 18. Erosion observed at final stage of the test. (a) Conventional type embankment (CASE A, 3 min after). (b) GRS embankment (CASE B, 10 min after).

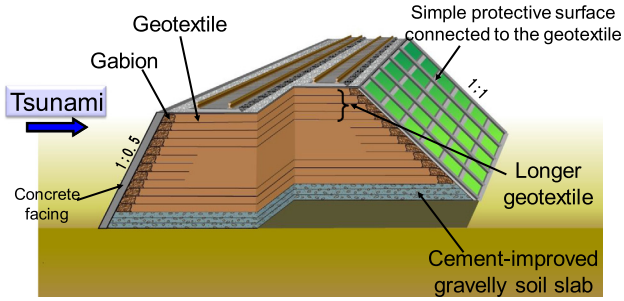

Fig. 19. Suggestion of new geotextile reinforced-soil embankment.

at the edges of the embankment. Furthermore, the outflow of the protective surface due to uplift pressure (negative pressure) during prolonged tsunami overflows can be prevented by integrating the protective surface with the geotextile.

The bottom layer of the embankment is constructed by the "cement-mixed gravelly soil slab" to prevent the erosion of the supporting ground from propagating to the embankment body.

It should be noted that another major advantage of applying the GRS method to an embankment is that the facing of the retaining wall or slope of the embankment can be constructed such that it is steeper than that in the conventional method without decreasing the stability of the earth structure especially during earthquakes. Extensive studies and a precise investigation after a severe earthquake have already indicated that the GRS structure will exhibit high seismic stability even if the wall or slope is steep. In addition to the advantages of the GRS structure itself, the study revealed the high resistance of the GRS structure relative to overflows. This indicates a significant practical advantage such that it is possible to construct an embankment with a high resistance to earthquakes and prolonged overflows at smaller sites compared to the conventional method.

Given that the collapse of river dikes and levees due to overflowing is typically reported during heavy rainfall events, the findings obtained in the present study (e.g., the practical advantages of GRS structures) are considered as being applicable to embankments as well as to river dikes and levees. Furthermore, the proposed method can be applied to both new constructions and to existing embankments or river dikes to reinforce them against overflowing by widening the landward side using the GRS method with less additional land acquisition.

5.2. Design procedure for GRS embankment

5.2.1. Design flow of GRS embankment

The design flow of the proposed structure is shown in Fig. 20. The design takes into consideration the levels of the external forces of the tsunami, in addition to those considered for ordinary designs (including seismic and non-seismic conditions). The external forces of a tsunami acting on an embankment and other relevant conditions are (1) the level of the sliding stability of the embankment with respect to the impact wave pressure during a tsunami, (2) the level of pullout or rupture of the reinforcement materials under the uplift pressure caused by tsunami overflows, and (3) the instability of the embankment that occurs when the supporting ground erodes. The design adopted cement-improved gravelly soil slabs to address this concern.

5.2.2. Mechanical effect of geotextile considered in design procedure

In the proposed design procedure (Fig. 20), the mechanical reinforcing effects of the geotextile are considered as follows.

(1) Improvement in the seismic stability of the embankment

The use of geotextile improves the seismic stability of the embankment and reduces the damage to the embankment body due to an earthquake. It raises the initial erosion resistance of the embankment against tsunamis. This effect is considered in "(1) General design of reinforced soil structure (seismic condition)" in Fig. 20.

(2) Prevention of the erosion of the embankment material

As shown in Fig. 3, due to the large negative pressure acting continuously on the slope of an embankment (land-

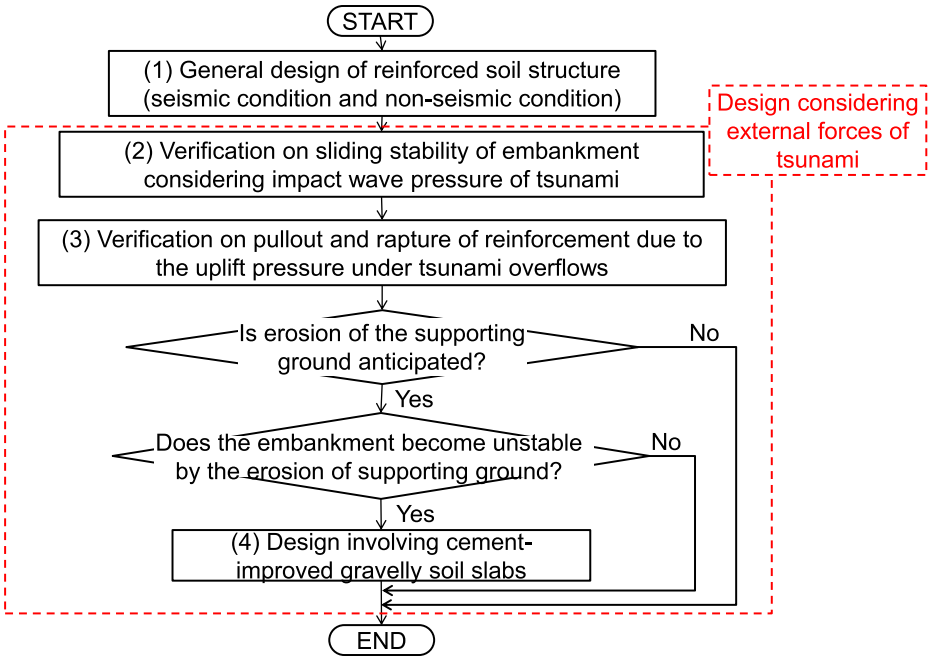

Fig. 20. Design flow of the proposed GRS embankment considering tsunami effect.

ward side), the erosion of the banking materials can easily occur especially around the top of the slope. In the present study, the geotextile was seen to effectively reduce the tractive force acting on the banking material, which increased the erosion resistance.

The magnitude and range of negative pressure (uplift pressure) acting on the slope of the embankment (landward side) can be calculated by the method proposed by Matsushima et al. (2014). The pullout and rupture of the reinforcement due to the uplift pressure was verified in the proposed design procedure ((3) in Fig. 20).

(3) Improvement in bending strength and stiffness of the cement-mixed gravely soil slab

The geotextile applied to the slab increases the bending strength and stiffness of the slab. The rupture of the reinforcement caused by the bending moment acting on the slab was verified in the proposed design procedure ((4) in Fig. 20).

6. Conclusion

In this study, small-scale and large-scale model tests were performed to propose a sturdy tsunami-resistant soil structure that exhibits ductile behavior relative to earthquakes prior to the onset of a tsunami and relative to prolonged overflowing. The following conclusions were obtained.

1. A conventional type of embankment with sufficient seismic stability can be rapidly eroded by overflowing. Erosion in the supporting ground accelerates the erosion of the embankment.
2. The GRS method is an effective measure against the erosion of the embankment due to overflowing. It is more effective to use the entire reinforcement (which is horizontally arranged from the left edge to the right edge of the embankment) to improve the durability and restorability of the embankment against prolonged overflowing.
3. Even if the embankment itself is stable, it can collapse due to the erosion of the supporting ground. An effective method for preventing such a collapse involves the partial improvement of the supporting ground immediately below the embankment and/or the application of a high-quality material or cement-mixed gravelly soil slab to the bottom layer of the embankment.
4. Based on the experimental results, an embankment structure with sufficient stability and ductility against large-scale earthquakes and prolonged overflows was developed by adopting the GRS method and applying a cement-mixed gravelly soil slab to the bottom layer of the embankment.
5. Several key points that must be considered when selecting the banking material for model tests have been summarized. Given that it is almost impossible to simultaneously satisfy all the points, the material should be carefully chosen by considering the purpose of the model tests and the behavior of the model on which the focus is placed.

The study addressed the tsunami overflows that occur after major earthquakes. However, the resisting performance of earth structures against prolonged overflows is of interest when tsunamis and severe rainstorms occur. Recently, there have been many incidents of railway embankments constructed in water catchments in mountainous areas and river basins that suffered from severe erosion caused by prolonged overflows. For example, during a

severe rainstorm that occurred in the Kyushu region in 2012, railway embankments constructed in the mountainous areas along the Ho-hi Line sustained extensive damage due to erosion caused by overflows. The GRS embankments that had been installed in the vicinity of the collapsed embankments sustained only minimal damage (Tatsuoka et al., 2014). In these cases, emphasis is always placed on water drainage measures and the protection of slopes when designing embankments against rainfall. The GRS structure proposed in the study is also useful in the construction of embankments in the aforementioned locations.

Furthermore, given that the collapse of river dikes and levees due to overflows is often reported during heavy rainfall events, the findings obtained in the present study (e.g., the practical advantages of GRS structures) are considered applicable to embankments as well as to river dikes and levees.

Acknowledgements

Technical advice and guidance for the technological development of this study were received from the Tokyo University of Science, the National Institute for Rural Engineering at the National Agriculture and Food Research Organization, and the Integrated Geotechnology Institute Limited through the joint research "Development of Structure Technology for Embankment Structures that are not Destroyed and Remain Steadfast Under a Tsunami" conducted from 2012 to 2013.

References

Chevalier, C., Pham Van Bang, D., Durand, E., Charles, I., Herrier, G., 2014. Scour and erosion phenomena occurring in waterways – recent advances. In: Proc. 7th Int. Conf. Scour and Erosion (ICSE7, Perth, Australia), ISBN: 978-1-315-72359-4, pp. 33–48.

Hatogai, S., Suwa, Y., Kato, F., 2012. Hydraulic model experiments on scour landward of the coastal dike induced by tsunami overflow. J. Japan Soc. Civil Eng., Ser. B2, Coastal Eng. 68 (2), I406–I410 (in Japanese).

Koseki, J., Koda, M., Matsuo, S., Takasaki, T., Fujiwara, T., 2012. Damage to railway earth structures and foundations caused by the 2011 off the Pacific Coast of Tohoku Earthquake. Soils Found. 52 (5), 872–889.

Lachaussée, F., Pham Van Bang, D., Vidal, V., Chevalier, C., Ndoye, O., Szymkiewicz, F., Minatchy, C., Martineau, F., Watanabe, K., 2016. Overflow erosion on mixed kaolin-sand embankments. Proc. of 8th International Conference on Scour and Erosion, pp. 653–657.

Lohani, T.N., Kongsukprasert, L., Watanabe, K., Tatsuoka, F., 2004. Strength and deformation properties of compacted cement-mixed gravel evaluated by triaxial compression tests. Soils Found. 44 (5), 95–108.

Japanese Geotechnical Society: Geo-hazards during earthquakes and mitigation measures-lessons and recommendations from the 2011 Great East Japan Earthquake, 2011. Available from: http://www.geosyntheticssociety.org/wp-content/uploads/2014/09/Japan_Earthquake.pdf (accessed 03.03.20).

Matsushima, K., Yamazaki, S., Mohri, Y., Hori, T., Ariyoshi, M., Tatsuoka, F., 2007. Large-scale overflow failure tests on embankments using soil bags anchored with geosynthetic reinforcement. Proc. of 5th Int. Sym. on Earth Reinforcement (IS Kyushu 2007), pp. 881–888.

Matsushima, K., Oi, K., Mohri, Y., Tatsuoka, F., Hirai, S., Kiri, H., 2014. Lift-up of cover-blocks of coastal dikes by overflowing tsunami current and counter-measure. J. Japan Soc. Civil Eng., Ser. B2, Coastal Eng. 70 (2) (in Japanese).

Miyamoto, K., Hirooka, A., Nagase, H., 2013. The influence on the embankment failure mechanisms of the ground erosion by Tsunami near the foot of its slope. Proc. of 48th Japan National Conference on Geotechnical Engineering (in Japanese).

Oda, A., Mizuyama, T., Miyamoto, K., Hasegawa, Y., 2007. The estimate method of erosion rate of cohesive materials. J. Japan Soc. Erosion Control Eng. 59 (5), 56–61 (in Japanese).

Pickert, G., Weitbrecht, V., Bieberstein, A., 2011. Breaching of overtopped river embankments controlled by apparent cohesion. J. Hydraul. Res. 49 (2), 143–156.

Powledge, G.R., Ralston, D.C., Miller, P., Chen, Y.H., Clopper, P.E., Temple, D.M., 1989a. Mechanics of overflow erosion on embankments. I.: research activities. J. Hydraul. Eng. 115 (8), 1040–1055.

Powledge, G.R., Ralston, D.C., Miller, P., Chen, Y.H., Clopper, P.E., Temple, D.M., 1989b. Mechanics of overflow erosion on embankments. II.: hydraulic and design considerations. J. Hydraul. Eng. 115 (8), 1056–1075.

Mizutani, H., Nakagawa, H., Yoden, T., Kawaike, K., Zhang, H., 2012. Numerical study on river embankment failure due to overtopping flow considering infiltration and mass sliding, Annuals of Disaster Prevention Research Institute, Kyoto Univ., No. 55B, (in Japanese).

Railway Technical Research Institute (RTRI): Design standards for railway structures and commentary (earth structures), 2007.

Suzuki, K., Tokida, K., Tanimoto, R., Akita, T., 2013. Experimental study on erosion characteristics on overflown embankment. Proc. of 48th Japan National Conference on Geotechnical Engineering (in Japanese).

Tabrizi, A.A., Elalfy, E., Elkholy, M., Chaudhry, M.H., Imran, J., 2017. Effects of compaction on embankment breach due to overtopping. J. Hydraul. Res. 55, 236–247.

Tatsuoka, F., Tateyama, M., Koseki, J., Yonezawa, T., 2014. Geosynthetic-Reinforced Soil Structures for Railways in Japan. Transportation Infrastructure Geotechnology, Springer 1 (1), 3–53.

Tokida, K., Tanimoto, R., 2012. Resistance of earth bank against tsunami and structure of dug pool formed by tsunami in the 2011 off the Pacific coast of Tohoku earthquake. J. Japan Soc. Civil Engineer, A1 68 (4), 1091–1112 (in Japanese).

Watanabe, K., Matsumaru, T., Tateyama, M., 2011. Soft ground improvement method for railway embankment using cement-mixed gravel and geosynthetic. Proc. of 1st International Symposium on Railway Geotechnical Engineering (Georail 2011), Paris, pp. 389–396.

Watanabe, K., Fujii, K., Matsuura, K., Nonaka. T., Kudo, A., Iijima, M., Yamaguchi, S., Aoyagi, Y., Daisuke, F., Kawabe, S., Kikuchi, Y., 2014. Hydraulic model tests on resistance characteristic of Geosynthetics-Reinforced soil against long term overtopping. Proc. of Special Symposium of Japanese Geotechnical Society, Tokyo, 2014. (in Japanese)

Watanabe, K., Nakajima, S., Fujii, K., Matsuura, K., Kudo, A., Nonaka, T., 2017. Development of railway embankment resistant to severe earthquakes and prolonged overflows caused by Tsunami. Proc. of 19th ICSMGE, Seoul, pp. 2937–2940.

Yamaguchi, S., Yanagisawa, M., Kawabe, S., Tatsuoka, F., Nihei, Y., 2013. Evaluation of the stability of various types of coastal dyke against over-flowing tsunami current. Proc. International Symposium on Design and Practice of Geosynthetic-Reinforced Soil Structures, Bologna (Ling et al., eds.), pp. 572–581.

Yamamoto, Y., Yoshino, F., 1978. The characteristics of slope failure of embankments by overtopping. Proc. of 33th Japan Society of Civil Engineers 1978 Annual Meeting (in Japanese).